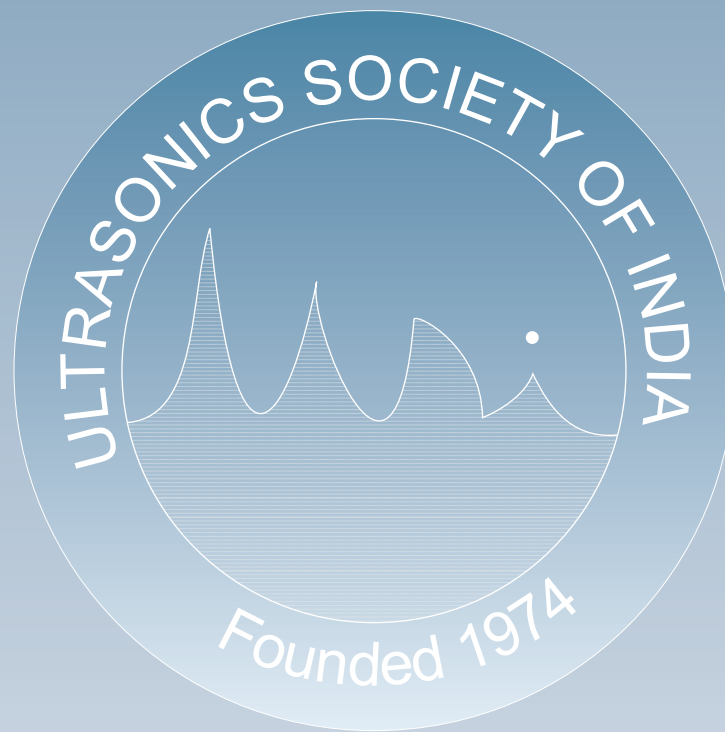


Journal of Pure and Applied
Ultrasonics

Including Transducers, Materials and Devices



Website : www.ultrasonicsindia.org

A Publication of Ultrasonics Society of India

Journal of Pure and Applied Ultrasonics

VOLUME 45

NUMBER 3-4

JULY-DECEMBER 2023

CONTENTS

Editorial S.K. Jain	42
Acoustical and stability studies on polyvinyl alcohol – A biodegradable polymer G.M. Rajesh, S. Jayakumar, N. Dharani Rajan, G.S. Gayathri and R. Ravi	43
Theoretical Investigation of Mechanical and Thermal Features in ScTiZr and ScTiHf Alloys: A Comparative Study Ramanshu P. Singh, Shakti Yadav, A.K. Tiwari and Giridhar Mishra	50
Design, modelling, construction and evaluation of a 64-element, 1 MHz ultrasonic probe R. Ramesh, P.P. Sathyanarayan, Monika Chaudhary, K.V. Lijin, T.K. Vinod Kumar, Sneha R.K. and A.J. Sujatha	60
Thermodynamic properties of curcumine with different alcohols and temperatures J. Jeya Priya, J. Poongodi, C. Duraivathi and K. Amudhavalli	72
Theoretical investigation on the effect of pressure on mechanical, thermo-physical and ultrasonic properties of La_2CO_3 Prashant Srivastav, Adwitiya Yadav, Vivek Chaurasiya, Aadesh Kumar Prajapati and Pramod Kumar Yadawa	79
Ph.D. Thesis Summary Dr. Kalpana Yadav under Dr. Sanjay Yadav, Academic of Scientific and Innovative research (AcSIR) CSIR-National Physical Laboratory New Delhi	88
A.K. Prajapati under Dr. Pramod Kumar Yadawa, Associate Professor Department of Physics Prof. Rajendra Singh (Rajju Bhaiya) Institute of Physical Sciences for Study and Research, Veer Bahadur Singh Purvanchal University, Jaunpur-222 003, India	89
Author Index	90

(Authors have stated that the papers have neither been published nor have been submitted for publication elsewhere)

Theoretical Investigation of Mechanical and Thermal Features in ScTiZr and ScTiHf Alloys: A Comparative Study

Ramanshu P. Singh^{1*}, Shakti Yadav¹, A.K. Tiwari^{2#} and Giridhar Mishra^{1#}

¹Department of Physics, Prof. Rajendra Singh (Rajju Bhaiya) Institute of Physical Sciences for Study and Research, Veer Bahadur Singh Purvanchal University, Jaunpur-222 001, Uttar Pradesh, India

²Department of Physics, BSNV PG College, Lucknow-226 001, Uttar Pradesh, India

*E-mail: ramanshupsingh@gmail.com

This research article presents the theoretical investigation to study the mechanical and thermal properties of hexagonal closed-packed structured ScTiZr and ScTiHf ternary alloys. Lennard-Jones potential model has been used to compute the second order and third order elastic constants (SOECs and TOECs). The study focuses on elastic properties such as elastic moduli, ultrasonic velocities in different directions of hexagonal closed-packed cell, thermal properties such as heat capacity, thermal energy density and lattice thermal conductivity and ultrasonic attenuation due to phonon-phonon interactions and thermo-relaxation mechanism. It has been found that ScTiHf has more stiffness and tensile strength than ScTiZr. Heat capacity follows Dulong-Petit law and ultrasonic attenuation due to phonon-phonon interactions is predominant over that due to thermo-relaxation mechanism.

Keywords: Ternary alloys, elastic and thermal properties, Lennard-Jones potential, ScTiZr and ScTiHf alloys, ultrasonic attenuation.

Introduction

In recent years, there has been a growing interest in the development and application of advanced alloys in various industries^{1,2}. One area of focus is the study of mechanical and thermal properties of alloys, as these properties play a crucial role in determining their suitability for industrial applications. The study of alloy properties is essential for understanding their behaviour under different conditions and for optimizing their performance in industrial applications. One aspect that significantly affects the properties of alloys is their crystallographic configuration^{3,4}. Substitutional solid solutions, such as alloys, can exist in both ordered and disordered states, leading to marked differences in their physical properties⁵. The ordering of alloys can result in major crystallographic reconfigurations, altering the atomic basis, symmetry, and periodicity of the material. In alloys, refractory high entropy alloys, composed of refractory metals such as Ti, Zr, Hf, Nb etc have been extensively explored for their excellent mechanical and thermal properties and industrial applications⁶⁻⁸.

ScTiHf and ScTiZr are two potential alloy systems that combine the individual properties of scandium (Sc), titanium (Ti), hafnium (Hf), and zirconium (Zr). Sc is the lightest transition metal with good thermal conductivity and tensile strength, while Ti, Hf, and Zr are excellent refractory metals known for their extraordinary mechanical and thermal properties, including high tensile strength, resistance to wear and tear, and high-temperature resistance.

The combination of these elements in ScTiHf and ScTiZr alloys offers the potential for enhanced mechanical and thermal properties compared to their individual constituents. Previous studies have investigated the effects of Sc and Y additions on the properties of HCP structured TiZrHf alloys and found improved strength and ductility in TiZrHfSc alloys compared to TiZrHf alloys⁹. Thermoelastic behaviour studies have also been conducted on ScTiZr, ScTiHf, ScZrHf, and ScTiZrHf alloys, evaluating various properties of these alloys¹⁰.

While there have been some experimental and theoretical studies on HCP structured high-entropy

Life member, Ultrasonic Society of India

alloys, there is still a lack of investigation into temperature-dependent elastic constants, thermal properties, and ultrasonic properties for HCP structured ScTiHf and ScTiZr alloys¹¹⁻¹³. Therefore, this research paper aims to fill this gap by utilizing a theoretical approach to determine temperature-dependent second-order elastic constants (SOECs), third-order elastic constants (TOECs), elastic moduli, Poisson's ratio, ultrasonic velocities, Debye average velocity, Debye temperature, thermal energy density, heat capacity, and ultrasonic attenuation for HCP structured ScTiHf and ScTiZr alloys.

By investigating the mechanical and thermal properties of ScTiHf and ScTiZr alloys, this research aims to provide valuable insights into the potential applications of these alloys in high-pressure and high-temperature environments. The results of this study can contribute to the optimization and development of these alloys for various industrial applications, such as aerospace, automotive, and energy sectors.

Theory

The theoretical approach used in this study involves the utilization of the Lennard-Jones potential method to compute the SOECs and TOECs at different temperatures for ScTiHf and ScTiZr alloys. The formulation for calculating the independent SOECs and TOECs can be found in the literature¹⁴⁻¹⁶. For computing SOECs and TOECs, temperature dependent lattice parameters were taken from the literature¹⁷. The bulk modulus, modulus of rigidity and Young's modulus are computed using the Voigt-Reuss-Hill method for hexagonal crystals^{18,19}.

Additionally, the ultrasonic velocities are important parameters for estimating the mechanical properties of materials¹. These velocities, including the longitudinal (V_L), quasi-shear (V_{S1}), and shear (V_{S2}) modes, can be calculated along different angles (θ) with the unique axis of a hexagonal close-packed (HCP) crystal²⁰ with following formulation:

$$V_L^2 = \frac{C_{33} \cos^2 \theta + C_{11} \sin^2 \theta + C_{44} + \left\{ \left(C_{11} \sin^2 \theta - C_{33} \cos^2 \theta + C_{44} (\cos^2 \theta - \sin^2 \theta) \right)^2 + 4 \cos^2 \theta \sin^2 \theta (C_{13} + C_{44})^2 \right\}^{\frac{1}{2}}}{2\rho} \quad (1)$$

$$V_{S1}^2 = \frac{C_{33} \cos^2 \theta + C_{11} \sin^2 \theta + C_{44} - \left\{ \left(C_{11} \sin^2 \theta - C_{33} \cos^2 \theta + C_{44} (\cos^2 \theta - \sin^2 \theta) \right)^2 + 4 \cos^2 \theta \sin^2 \theta (C_{13} + C_{44})^2 \right\}^{\frac{1}{2}}}{2\rho} \quad (2)$$

$$V_{S2}^2 = \frac{C_{44} \cos^2 \theta + C_{166} \sin^2 \theta}{\rho} \quad (3)$$

$$V_D = \left[\frac{1}{3} \left(\frac{1}{V_L^3} + \frac{1}{V_{S1}^3} + \frac{1}{V_{S2}^3} \right) \right]^{\frac{1}{3}} \quad (4)$$

Where C_{IJ} are SOECs. The Debye average velocity (V_D) and Debye temperature (θ_D) are determined using these ultrasonic velocities^{14,20,21} as follows:

$$\theta_D = \frac{h}{k_B} \left(\frac{3n}{4\pi} \frac{N\rho}{M} \right)^{\frac{1}{3}} V_D \quad (5)$$

Additionally, the Debye model for heat capacity is utilized to evaluate the heat capacity (C_V) and thermal energy density (E_o) of medium-entropy alloys at various temperatures (T)²² with the help of following formulation:

$$C_V = 9Nk_B \left(\frac{T}{\theta_D} \right)^3 \int_0^{\theta_D/T} \frac{x^4 e^x}{(e^x - 1)^2} dx \quad (6)$$

$$E_o = 9Nk_B T \left(\frac{T}{\theta_D} \right)^3 \int_0^{\theta_D/T} \frac{x^3}{e^x - 1} dx \quad (7)$$

The thermal properties, such as heat capacity, thermal energy density, and thermal conductivity, are important to investigate for potential materials used in high pressure and temperature conditions. These properties provide valuable information about the future performance of the materials²². For lattice thermal conductivity, Morelli and Slack²³ have deduced theoretical formulation as below:

$$\kappa = A \frac{M_a \theta_D^3 \delta}{\gamma^2 T n^{2/3}} \quad (8)$$

where δ is the cube root of volume per atom (in \AA^3), n is the number of atoms per unit cell, M_a (in amu) is average atomic mass, T is the temperature (in K), γ is Grüneisen constant and A is a proportionality constant.

The mechanical properties of solid and liquid materials, such as elastic moduli, mechanical stability, thermal conductivity, and heat capacity, are closely related to ultrasonic attenuation²⁴. At high temperatures, the main causes of ultrasonic attenuation in solids are phonon-phonon interaction also known as Akhiezer loss and loss due to thermo-elastic relaxation

mechanism²⁴⁻²⁶. The formulation for evaluating the ultrasonic absorption coefficient over frequency squared (αf^2) due to phonon-phonon interaction for longitudinal and shear modes has been developed by Mason and Bateman^{27,28}. This formulation takes into account parameters such as the acoustic coupling constant (D), ultrasonic velocity (V), square average and average square Grüneisen numbers ($\langle\langle\gamma_i^j\rangle\rangle$ and $\langle\gamma_i^j\rangle^2$) and thermal relaxation time $th = \frac{3\kappa}{C_v V_D^2}$ and is given as follows:

$$\left(\frac{\alpha}{f^2}\right) = \frac{4\pi^2 \tau_{th} E_o D}{2\rho V^3} \quad (9)$$

$$D = 9\langle\langle\gamma_i^j\rangle\rangle - \frac{3\langle\gamma_i^j\rangle^2 C_v T}{E_o} \quad (10)$$

Additionally, the ultrasonic attenuation due to thermo-relaxation mechanism can be computed using the Grüneisen numbers, temperature (T), thermal conductivity (κ), and longitudinal ultrasonic velocity (V_L)²⁹:

$$\left(\frac{\alpha}{f^2}\right)_{th} = \frac{4\pi^2 \langle\gamma_i^j\rangle^2 \kappa T}{2\rho V_L^5} \quad (11)$$

These relationships provide valuable insights into the behaviour of materials under ultrasonic waves and contribute to the understanding of their mechanical properties.

Results and Discussion

Mechanical Properties : The Fig. 1 depicts the estimated SOECs and TOECs for ScTiHf and ScTiZr in

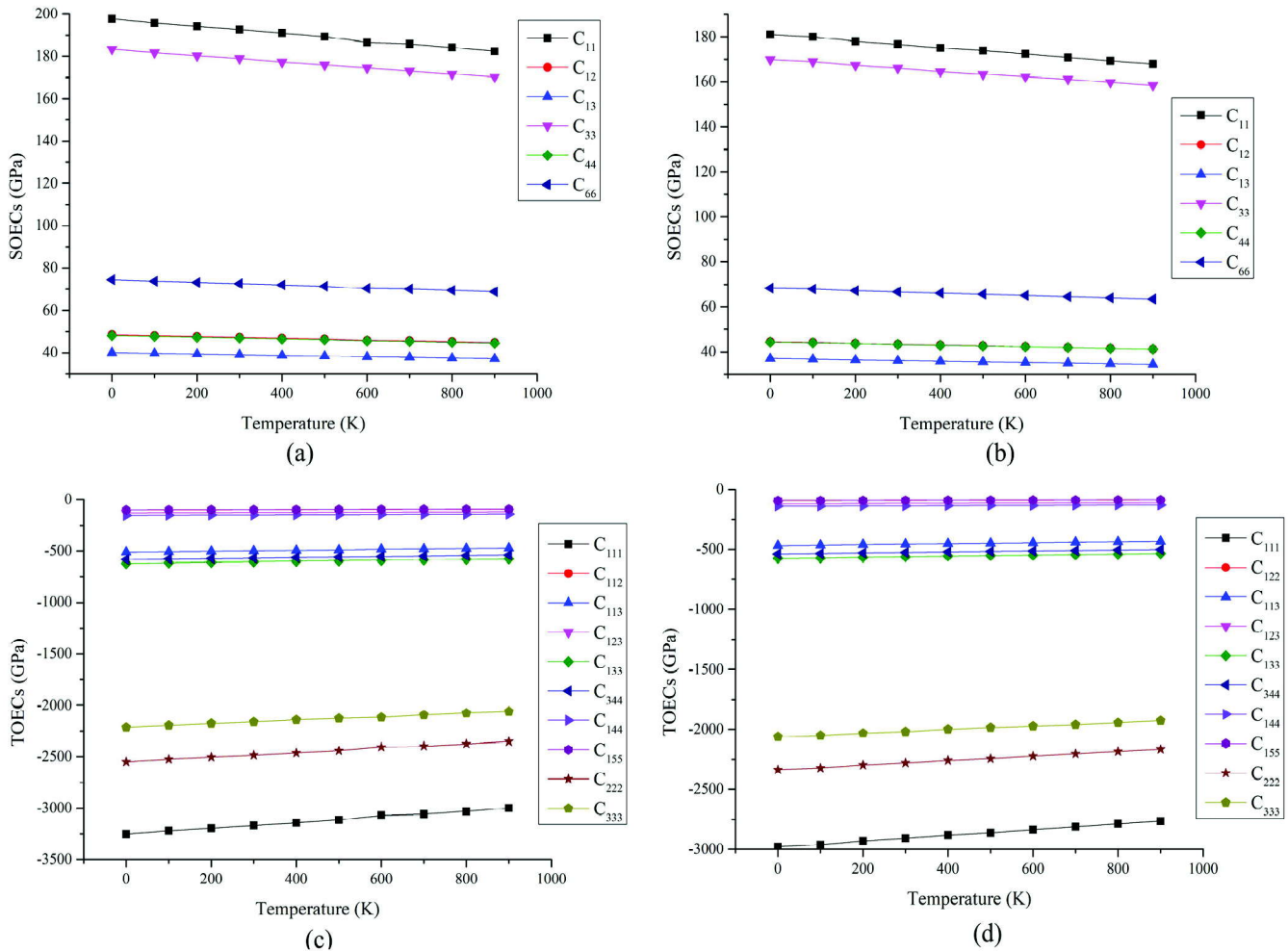


Fig. 1. Temperature dependent SOECs of (a) ScTiHf, (b) ScTiZr and TOECs of (c) ScTiHf and (d) ScTiZr in GPa

the temperature range of 0K-900K. It is well shown in the figure that the SOECs and TOECs for both the material show the similar effect of decrement with increase in temperature but the SOECs for ScTiHf are higher in comparison to that of ScTiZr. TOECs for both the alloys have negative values confirming a distinct relationship between direction of applied stress and deformity in different directions³⁰.

The temperature dependence of different moduli for both of the alloys has been shown in the Fig. 2. The elastic moduli for ScTiHf are higher than that of ScTiZr. With this, it can be said that ScTiHf have higher tensile strength than ScTiZr. It is also clear from the figure that all the moduli decrease with increase in temperature. This could be related to increased lattice vibrations and deformation due to high temperature³¹.

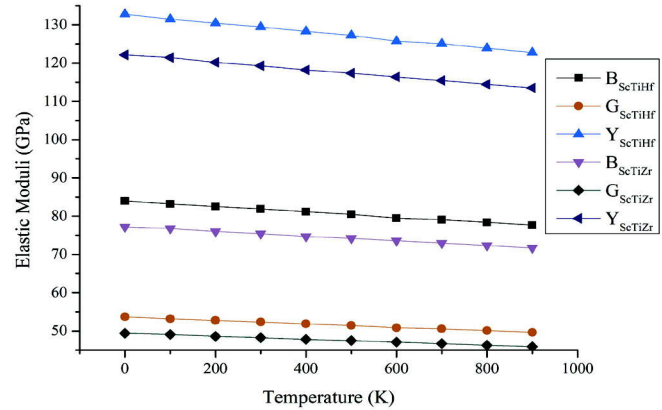


Fig. 2. Temperature dependent Bulk modulus (B), modulus of rigidity (G) and Young's modulus (Y) in GPa

Ultrasonic velocities in longitudinal (V_L), quasi-shear (V_{S1}) and shear (V_{S2}) modes of vibrations and Debye

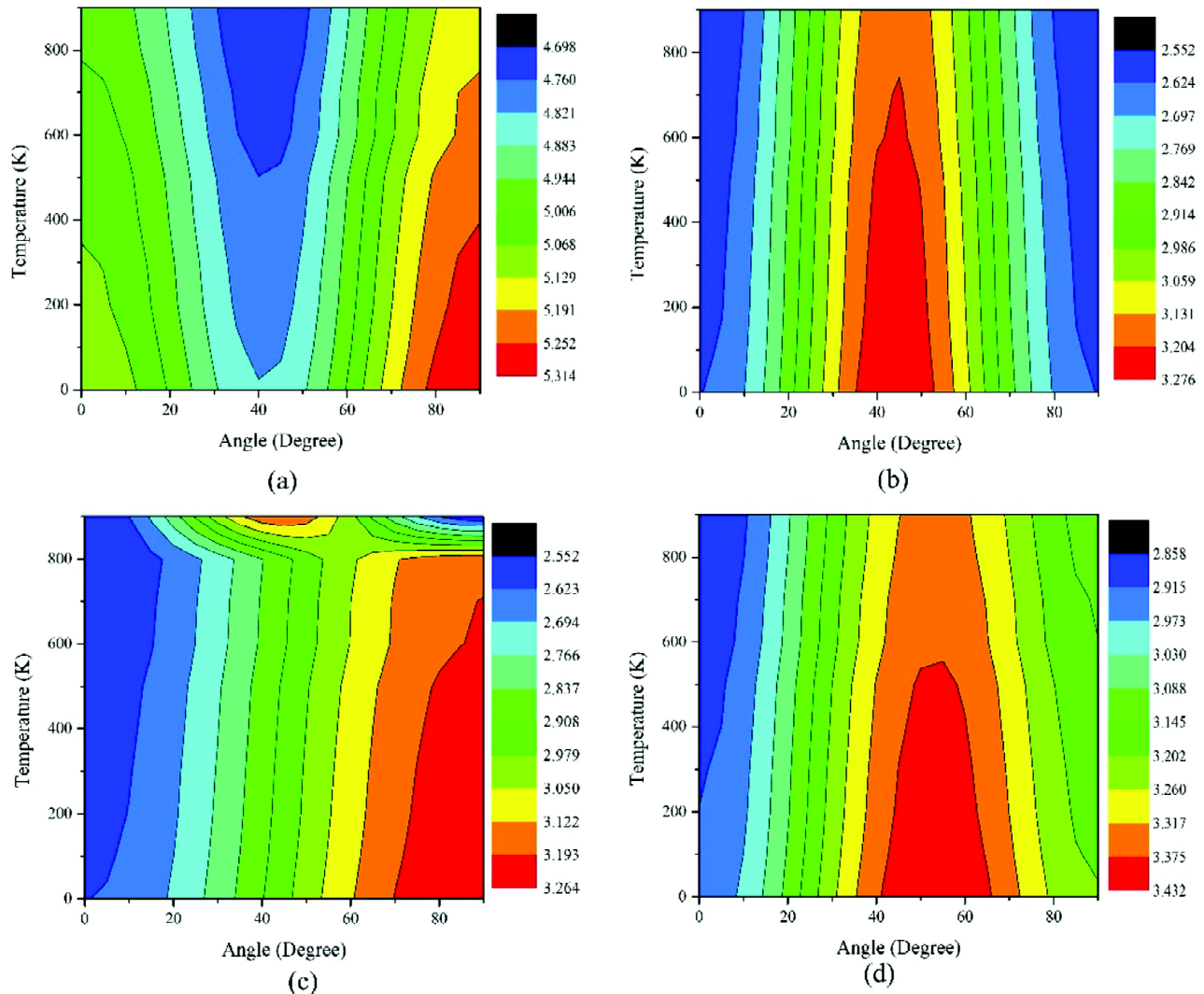


Fig. 3. Temperature and direction dependent ultrasonic velocities in (a) longitudinal, (b) quasi-shear, (c) shear modes of vibration and (d) Debye average velocity in 10^3 m/s for ScTiHf

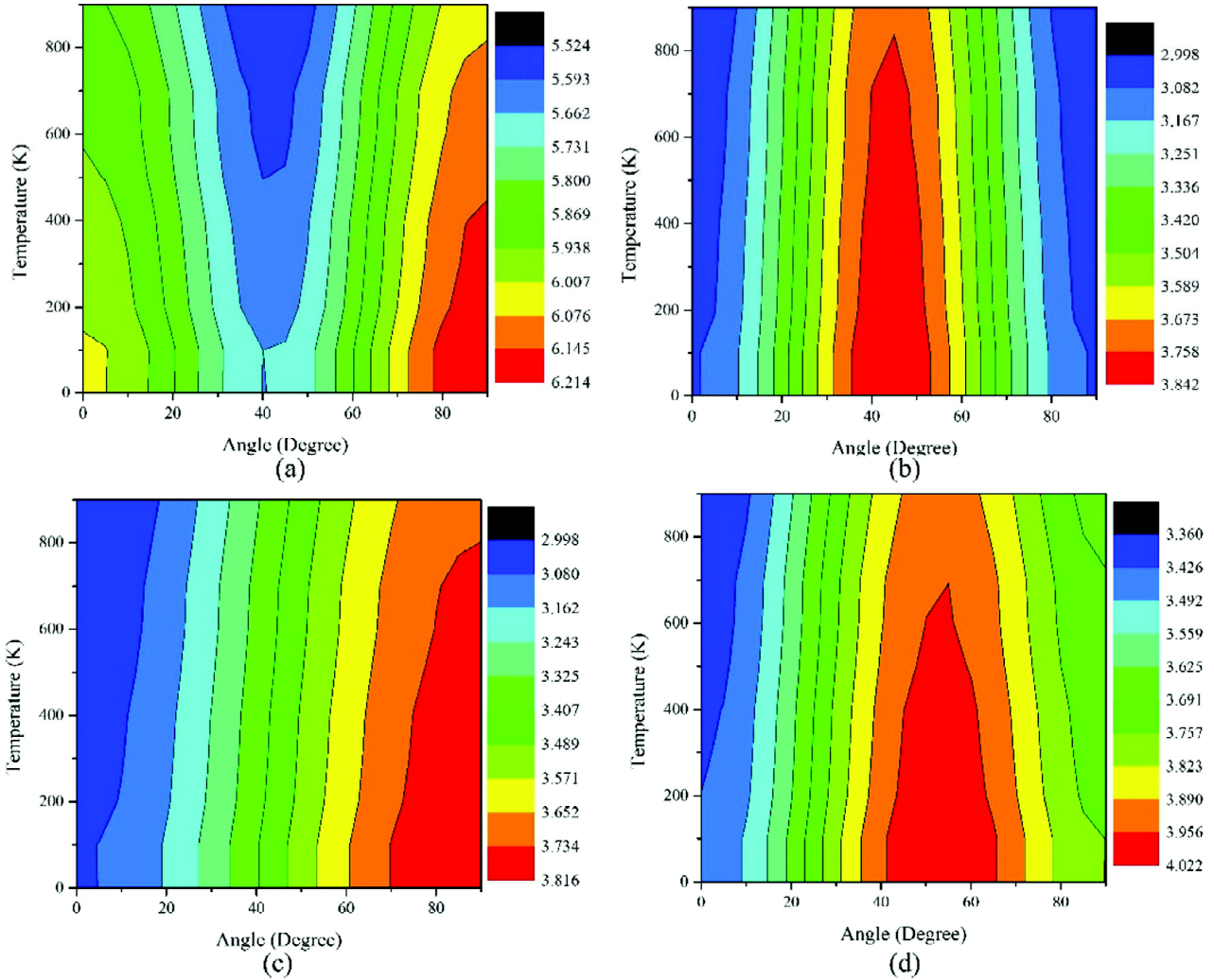


Fig. 4. Temperature and direction dependent ultrasonic velocities in (a) longitudinal (V_L), (b) quasi-shear (V_{SL}), (c) shear (V_{S2}) modes of vibrations and (d) Debye average velocity in 10^3 m/s for ScTiZr

average velocity (V_D) at different angle with unique axis of the HCP crystal in the temperature range of 0-900K have been evaluated for ScTiHf and ScTiZr by following the formulation given by equations (1)-(4) and presented in the Fig. 3 and Fig. 4 respectively.

For ScTiHf, the longitudinal wave velocity V_L reduces as temperature rises, but it also lowers as angle rises up to 45° with the special axis and then begins to rise once more from 45° to 90° . The highest velocity at 90° and 0K is 5.31×10^3 m/s. Although, quasi-shear wave velocity (V_{SL}) also declines with temperature, it has a maximum value of 3.27×10^3 m/s at a 45° angle.

Temperature causes a monotonic drop in the shear velocity V_{S2} , whereas angle causes an increase. The maximum value of 3.43×10^3 m/s at 0 K temperature and angle = 55° is displayed by the Debye average

velocity V_D , which exhibits characteristics comparable to quasi-shear wave velocity.

Fig. 4 clearly shows that the longitudinal wave velocity V_L of ScTiHf decreases as temperature rises, but it also decreases as angle climbs up to 45° with the unique axis and then begins to rise again from 45° to 90° . At 90° and 0 K, the maximum velocity (V_L) is 6.21×10^3 m/s. Although the quasi-shear wave velocity (V_{SL}) decreases with temperature, it reaches a maximum of 3.84×10^3 m/s at a 45° angle. Temperature induces a monotonic decrease in V_{S2} , whereas angle generates an increase. The Debye average velocity V_D , which exhibits features similar to quasi-shear wave velocity, has a maximum value of 4.02×10^3 m/s at 0 K temperature and angle = 55° .

Though, these velocities could not be verified due to

unavailability in the literature, we could find a fair agreement of HCP alloys' ultrasonic velocity values when comparing to those of other HCP metals and alloys in literature^{26,32,33}.

Thermal Properties : The Debye temperature for ScTiHf and ScTiZr alloys decrease from 314.68 K to 303.96 K and 367.53 K to 355.85 K respectively with increase in temperature from 0-900K. The heat capacity (C_V) and thermal energy density (E_ρ) at different temperatures for both alloys have been computed using Debye temperature following equations (6)-(7) and plotted in the Fig. 5. The heat capacity, initially increases with temperature but becomes almost constant at higher temperature confirming the Dulong-Petit law³⁴ and thermal energy density shows a linear increment with temperature.

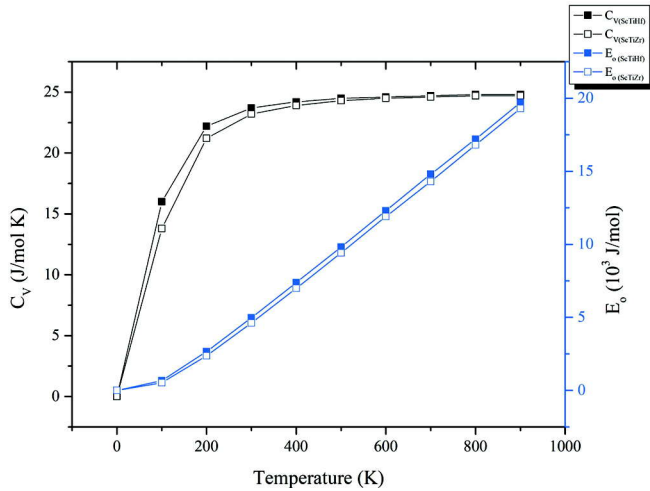


Fig. 5. Heat capacity (C_V) and thermal energy density (E_ρ) at different temperatures for ScTiHf and ScTiZr.

Study of thermal conductivity not only provide insight into the mechanisms governing heat transfer in complex materials, but also leads to advancement in our understanding of phonon transport, lattice dynamics, and thermal transport phenomena in alloys. In addition, it helps in the design and development of new materials with tailored thermal properties. Considering these merits, the lattice thermal conductivity for ScTiHf and ScTiZr at different temperatures along the unique axis has been evaluated using equation (8) and presented in the Fig. 6. The lattice thermal conductivity decreases with increase in temperature and is 10.41 W/mK for ScTiHf and 13.07 W/mK ScTiZr at 300K. The decrease in lattice thermal conductivity with increasing temperature can be attributed to increased phonon-

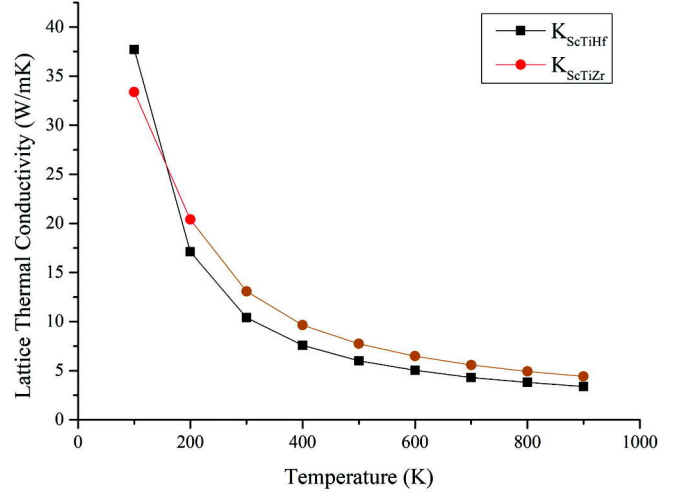


Fig. 6. Lattice Thermal Conductivity of ScTiHf and ScTiZr at different temperatures

phonon scattering at high temperature³⁵. At lower temperatures, the thermal conductivity of ScTiHf is higher than that of ScTiZr but becomes slightly lesser than that of ScTiZr at 300 K and higher temperatures.

Ultrasonic attenuation : The main objective of the present study is to investigate the ultrasonic behaviour of the metal alloys ScTiHf and ScTiZr. This is because the ultrasonic attenuation is directly related to the thermoelastic properties of the material³⁶. The study focuses on two types of ultrasonic attenuation: Akhiezer loss, which is caused by phonon-phonon interaction, and thermoelastic relaxation. These types of attenuation are of particular interest because they have a significant impact on the material's properties at high temperatures (>100 K)^{36,37}. The ultrasonic attenuations for ScTiHf and ScTiZr have evaluated using equations (9)-(11) and presented in Fig. 7 and Fig. 8 respectively.

The ultrasonic attenuation in the longitudinal mode, denoted as $(\alpha/f^2)_L$, increases with increase in temperature but exhibits its highest value of 353.87×10^{-17} Np s²/m for ScTiHf 296.75×10^{-17} Np s²/m for ScTiZr at a temperature of 900 K and an angle of 45° with the unique axis. Previous research has suggested that the dominant form of attenuation is due to phonon-phonon interaction, surpassing other forms such as thermo-elastic relaxation³⁸. This is further supported by the plots in Fig. 7 and Fig. 8, which clearly demonstrate this trend.

The ultrasonic attenuation in shear modes of vibration presented in plot (b) of Fig. 7 and Fig. 8 for ScTiHf and ScTiZr, respectively increases with increase in

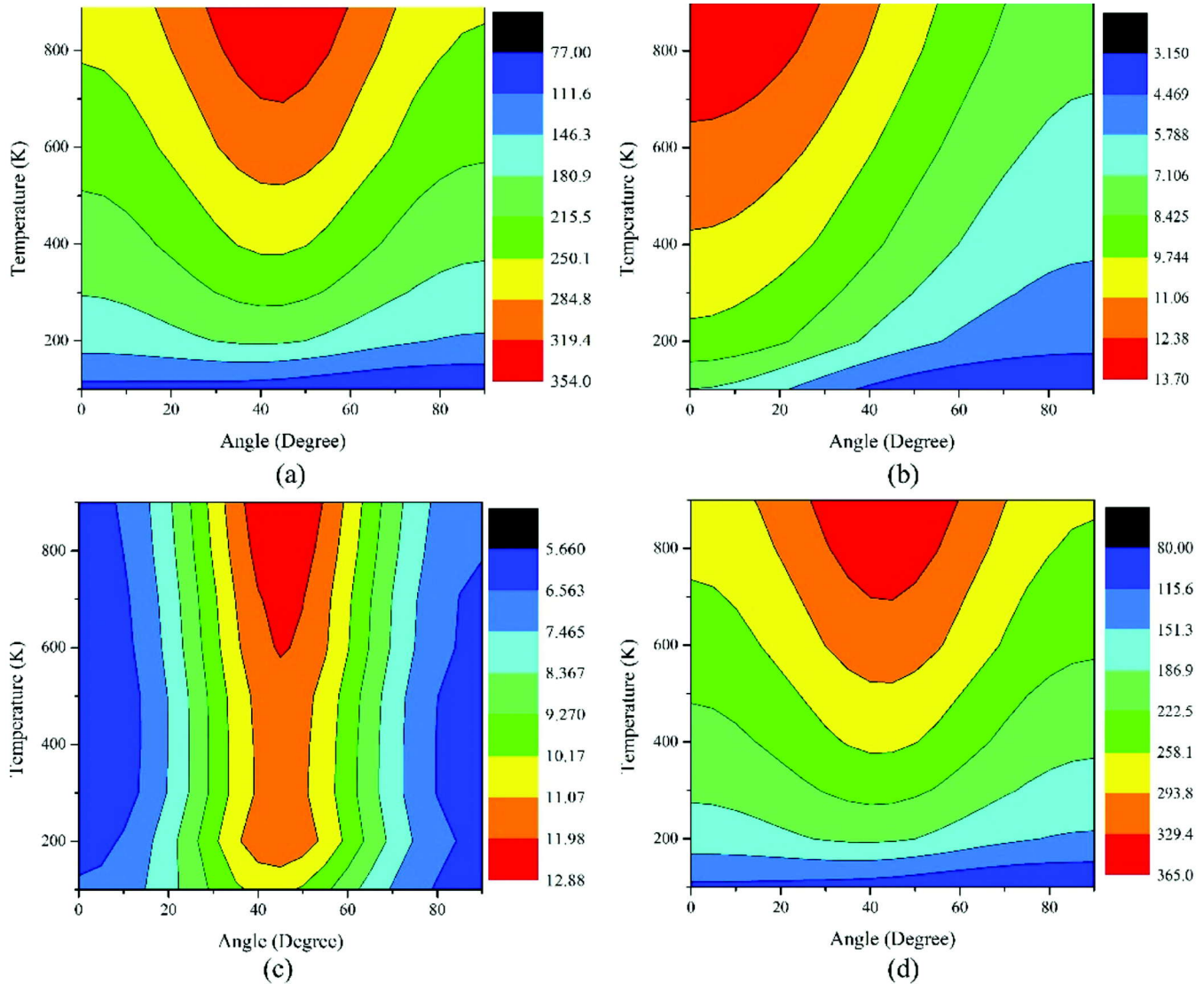


Fig. 7. Temperature and direction dependent Ultrasonic attenuation in (a) longitudinal (10^{-17} Np s²/m), (b) shear (10^{-17} Np s²/m), (c) due to thermo-relaxation mechanism (10^{-24} Np s²/m), and (d) total attenuation (10^{-17} Np s²/m) for ScTiHf

temperature but shows decrement with increase in angle with unique axis. The ultrasonic attenuation resulting from thermo-relaxation mechanism also depicts similar trend to the ultrasonic attenuation in longitudinal waves but the direction is much more dominant in the case of thermo-relaxation mechanism and the attenuation is in range of 10^{-24} Np s²/m, which again confirms that the phonon-phonon interaction dominates.

The total attenuation is sum of the ultrasonic attenuation due to phonon-phonon interactions including both longitudinal and shear modes of vibrations and due to thermo-relaxation mechanism. It is already established that the attenuation in longitudinal modes of vibrations is much higher than other type of

attenuations, therefore the total attenuation, also, follow the trend of ultrasonic attenuation in longitudinal waves as presented in the plot (d) of Fig. 7 and Fig. 8 for ScTiHf and ScTiZr ternary alloys.

Conclusion

The following important conclusions have been drawn on the basis of results in our investigation:

- The results are in good agreement with the available literature and thus, signify the importance and applicability of the Lennard-Jones potential model employed in this study.
- ScTiHf have more stiffness and tensile strength

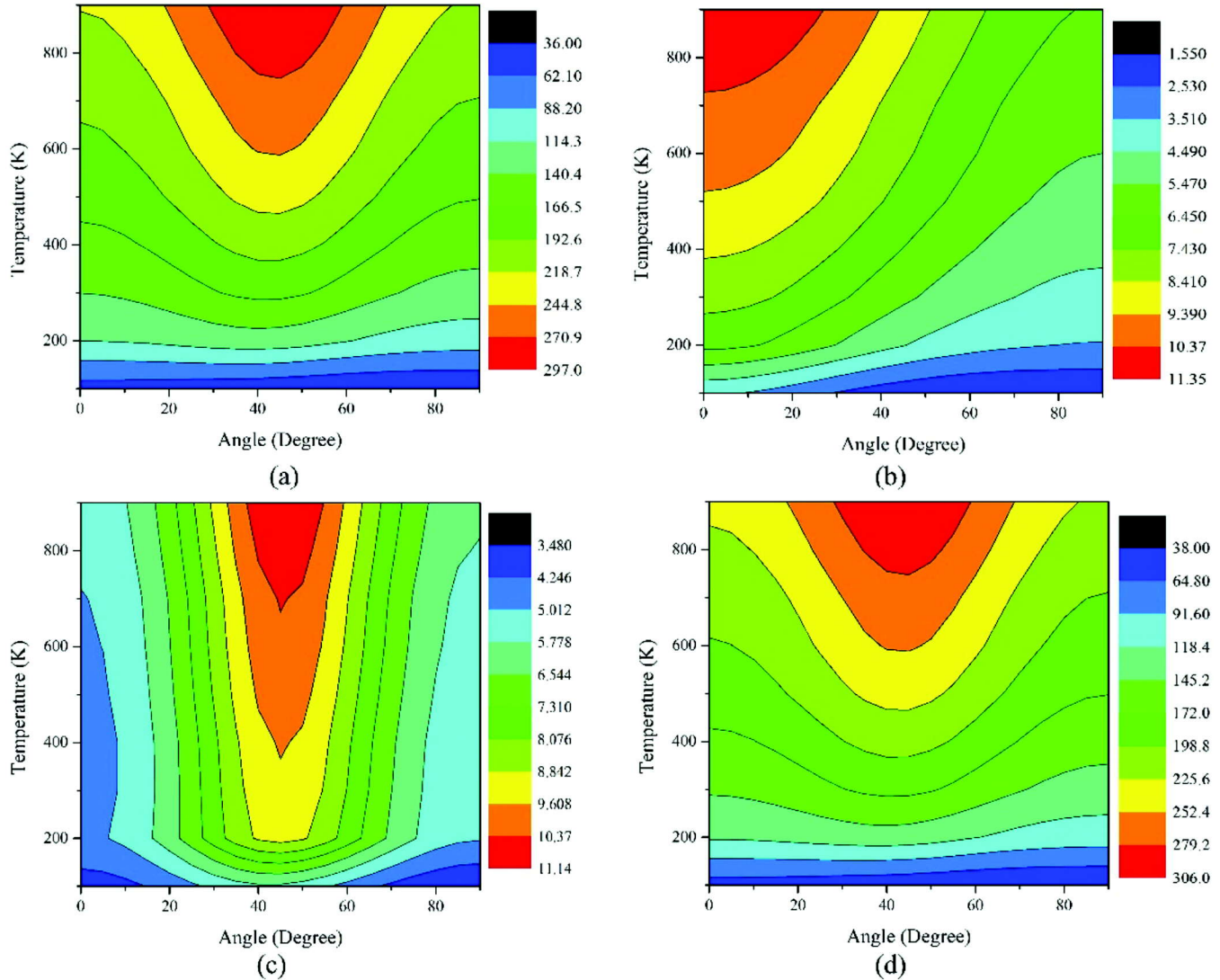


Fig. 8. Temperature and direction dependent Ultrasonic attenuation in (a) longitudinal (10^{-17} Np s²/m), (b) shear (10^{-17} Np s²/m), (c) due to thermo-relaxation mechanism (10^{-24} Np s²/m) and (d) total attenuation (10^{-17} Np s²/m) for ScTiZr

than ScTiZr.

- Heat capacity of both the alloys shows similar trend with temperature and follow Dulong-Petit law.
- The thermal conductivity of ScTiHf is greater than that of ScTiZr at lower temperature but at 300K and above, the thermal conductivity of ScTiZr is slightly greater than that of ScTiHf.
- The ultrasonic attenuation in ScTiHf is greater than that in ScTiZr.
- For both of the alloys, the ultrasonic attenuation in longitudinal modes of vibrations is found to be predominant over attenuation in the shear mode of vibration and thermoelastic relaxation mechanism.

Acknowledgement

One of us (SY) is thankful to *Council for Scientific and Industrial Research - Human Resource Development Group (CSIR-HRDG)* for providing financial support in the form of CSIR-Senior Research Fellowship (09/1014(0012)/2019-EMR-I).

References

1. **Gali A. and George E.P.**, Tensile properties of high- and medium-entropy alloys, *Intermetallics*, **39**, (2013) 74-78.
2. **Tsai Ming Hung and Yeh Jien Wei**, High-entropy alloys: A critical review, *Mater. Res. Lett.*, **2**(3), (2014) 107-123.
3. **Wang William Yi, Shang Shun Li, Wang Yi, Han**

- Fengbo, Darling Kristopher A., et al.**, Atomic and electronic basis for the serrations of refractory high-entropy alloys, *npj Comput. Mater.*, **3**(1), (2017) 23.
4. **Mishra Sumeet, Kulkarni Kaustubh, and Gurao N.P.**, Effect of crystallographic texture on precipitation induced anisotropy in an aluminium magnesium silicon alloy, *Mater. Des.*, **87**, (2015) 507-519.
 5. **Duda John C., English Timothy S., Jordan Donald A., Norris Pamela M. and Soffa William A.**, Reducing thermal conductivity of binary alloys below the alloy limit via chemical ordering, *J. Phys. Condens. Matter*, **23**(20), (2011) 205401.
 6. **Li Rui-Xuan, Qiao Jun-Wei, Liaw Peter K. and Zhang Yong**, Preternatural Hexagonal High-Entropy Alloys: A Review, *Acta Metall. Sin. English Lett.*, **33**(8), (2020) 1033-1045.
 7. **Chen Qizhi and Thouas George A.**, Metallic implant biomaterials, *Mater. Sci. Eng. R Reports*, **87**, (2015) 1-57.
 8. **Maiti Soumyadipta and Steurer Walter**, Structure and Properties of Refractory High-Entropy Alloys, In: TMS 2014: 143rd Annual Meeting & Exhibition, *Springer International Publishing, Cham*, (2014) 1093-1096.
 9. **Li Ruiqing, Dong Fang, Zhang Yun, Chen Pinghu and Li Xiaoqian**, Eutectic Phase Characterization and Mechanical Properties of Al-Cu Alloy Ingot Solidified With Ultrasonic Treatment, *Materials (Basel)*, (2022).
 10. **Obodo Kingsley Onyebuchi and Chetty Nithaya, A** Theoretical Study of Thorium Titanium-Based Alloys, *J. Nucl. Mater.*, (2013).
 11. **Yan Qing-song, Lu Gang, Luo Gui-ming, Xiong Bowen, and Zheng Qiangqiang**, Effect of synergistic action of ultrasonic vibration and solidification pressure on tensile properties of vacuum counter-pressure casting aluminum alloy, **15**(6), (2018) 411-417.
 12. **Xue Haitao, Li Di, and Ye Gang**, Ultrasonic Effects on Microstructure Evolution and Mechanical Properties of AZ80 Magnesium Alloy, *Rare Met. Mater. Eng.*, (2016).
 13. **Yusuf Sukaina Iskandar, Meteab Mohammed Muhana, and Annaz Abdulkader Ahmed**, Crystal Diffraction Techniques Were Used to Investigate the Structural Properties of Some Aluminum Alloys., *IOP Conf. Ser. Earth Environ. Sci.*, **961**(1), (2022) 012018.
 14. **Yadawa Pramod Kumar, Pandey Dharmendra Kumar, Singh Devraj, Yadav Raja Ram and Mishra Giridhar**, Computations of ultrasonic parameters of lanthanide metals Ti, Zr and Hf, *Turkish J. Phys.*, **34**(1), (2010) 23-31.
 15. **Singh Shakti Pratap, Singh Gaurav, Verma A. K., Jaiswal A.K. and Yadav R.R.**, Mechanical, Thermophysical, and Ultrasonic Properties of Thermoelectric HfX₂ (X = S, Se) Compounds, *Met. Mater. Int.*, **2**, (2020) 1-9.
 16. **Jyoti Bhawan, Singh Shakti Pratap, Gupta Mohit, Tripathi Sudhanshu, Singh Devraj, et al.**, Investigation of zirconium nanowire by elastic, thermal and ultrasonic analysis, *Zeitschrift für Naturforsch. A*, **75**(12), (2020) 1077-1084.
 17. **Huang Shuo, Cheng Jie, Liu Lei, Li Wei, Jin Hongyun, et al.**, Thermo-elastic behavior of hexagonal Sc-Ti-Zr-Hf high-entropy alloys, *J. Phys. D. Appl. Phys.*, **55**(23), (2022) 235302.
 18. **Hill R.**, Elastic properties of reinforced solids: Some theoretical principles, *J. Mech. Phys. Solids*, **11**(5), (1963) 357-372.
 19. **Saidi F., Benabadji M. K., Faraoun H. I. and Aourag H.**, Structural and mechanical properties of Laves phases YCu₂ and YZn₂: First principles calculation analyzed with data mining approach, *Comput. Mater. Sci.*, **89**, (2014) 176-181.
 20. **Yadawa Pramod K.**, Computational Study of Ultrasonic Parameters of Hexagonal Close-Packed Transition Metals Fe, Co, and Ni, *Arab. J. Sci. Eng.*, (2011).
 21. **Debye P.**, Zur Theorie der spezifischen Wärmen, *Ann. Phys.*, **344**(14), (1912) 789-839.
 22. **Singh Devraj, Mishra Giridhar, Kumar Raj and Yadav Raja Ram**, Temperature Dependence of Elastic and Ultrasonic Properties of Sodium Borohydride, *Commun. Phys.*, **27**(2), (2017) 151.
 23. **Morelli Donald T. and Slack Glen A.**, High Lattice Thermal Conductivity Solids, In: *High Thermal Conductivity Materials*, edited by Shindé S.L., Goela J.S., (Springer-Verlag, New York), (2006), 37-68.
 24. **Choi Sungho, Ryu Juyoung, Kim Jae-Seung and Jhang Kyung-Young**, Comparison of Linear and Nonlinear Ultrasonic Parameters in Characterizing Grain Size and Mechanical Properties of 304 L Stainless Steel, *Metals (Basel)*, **9**(12), (2019) 1279.
 25. **Akhiezer A.**, On the Absorption of Sound in Solids, *J. Phys.*, **1**(1), (1939) 277-287.
 26. **Singh Ramanshu P., Yadav Shakti, Singh Devraj and Mishra Giridhar**, Theoretical Approach to Investigate Temperature Dependent Ultrasonic and Thermophysical Properties of Ti-Zr-Hf Ternary Alloy, *Int. J. Res. Appl. Sci. Eng. Technol.*, **10**(11), (2022) 583-588.
 27. **Mason Warren P. and Bateman T.B.**, Ultrasonic-Wave Propagation in Pure Silicon and Germanium, *J. Acoust. Soc. Am.*, **36**(4), (1964) 644-652.
 28. **Shakti Yadav, Singh Ramanshu P., Singh Devraj and Mishra Giridhar**, Investigation of temperature dependent mechanical, thermophysical and ultrasonic properties of ScZrHf ternary alloy, *J. Pure Appl. Ultrason.*, **44**(3-4), (2022) 79-85.

29. **Wang S.Y. and Chen B.J.**, The Flakes Alignment Efficiency and Orthotropic Properties of Oriented Strand Board, *55*(1), (2001) 97-103.
30. **Takahashi Sennosuke**, Measurement of third-order elastic constants and stress dependent coefficients for steels, *Mech. Adv. Mater. Mod. Process.*, **4**(1), (2018) 2.
31. **SUZUKI Isao and ANDERSON Orson L.**, Elasticity and thermal expansion of a natural garnet up to 1,000 K., *J. Phys. Earth*, **31**(2), (1983) 125-138.
32. **Rai Sachin, Chaurasiya Navin and Yadawa Pramod K.**, Elastic, Mechanical and Thermophysical properties of Single-Phase Quaternary ScTiZrHf High-Entropy Alloy, *Phys. Chem. Solid State*, **22**(4), (2021) 687-696.
33. **Singh Ramanshu P.**, Yadav Shakti, Mishra Giridhar, and Singh Devraj, Pressure dependent ultrasonic properties of hcp hafnium metal, *Zeitschrift fur Naturforsch. - Sect. A J. Phys. Sci.*, **76**(6), (2021) 549-557.
34. **Tari A. and Tari I.**, Dulong-Petit Law and the Specific Heat Capacity of Solids, *J. Chem. Educ.*, **94**(2), (2017) 162-166.
35. **Nagarjuna S.**, Thermal conductivity of Cu-4.5 Ti alloy, *Bull. Mater. Sci.*, **27**(1), (2004) 69-71.
36. **Giordano Valentina M., Datchi Frédéric and Dewaele Agnès**, Melting curve and fluid equation of state of carbon dioxide at high pressure and high temperature, *J. Chem. Phys.*, **125**(5), (2006).
37. **Jyoti Bhawan, Triapthi Sudhanshu, Singh Shakti Pratap, Singh D.K. and Singh Devraj**, Elastic, mechanical, thermo-physical, and ultrasonic investigation in platinum carbide, *Mater. Today Commun.*, **27**, (2021) 102189.
38. **Kor S.K. and Singh R.K.**, Ultrasonic Attenuation in Alloys, *Acta Phys. Pol. A*, **83**(6), (1993) 751-758.